Title

Attenuating M-current suppression in vivo by a mutant Kcnq2 gene knock-in reduces seizure burden and prevents status epilepticus–induced neuronal death and epileptogenesis

Journal

Epilepsia, 59(10)

ISSN

0013-9580

Authors

Greene, Derek L
Kosenko, Anastasia
Hoshi, Naoto

Publication Date

2018-10-01

DOI

10.1111/epi.14541

Peer reviewed

HHS Public Access

Author manuscript

Epilepsia. Author manuscript; available in PMC 2019 October 01.

Published in final edited form as:

Epilepsia. 2018 October ; 59(10): 1908–1918. doi:10.1111/epi.14541.

Attenuating M-current suppression *in vivo* by a mutant *Kcnq2* gene knock-in reduces seizure burden, and prevents status epilepticus-induced neuronal death and epileptogenesis

Derek L. Greene[1], **Anastasia Kosenko**[1], and **Naoto Hoshi**[1,2,*]

[1]Department of Pharmacology, University of California, Irvine.

[2]Department of Physiology and Biophysics, University of California, Irvine.

SUMMARY

Objectives: The M-current is a low threshold voltage-gated potassium current generated by Kv7 subunits that regulates neural excitation. Importantly, M-current suppression, induced by activation of Gq-coupled neurotransmitter receptors, can dynamically regulate the threshold of action potential firing and firing frequency. Here we sought to directly examine whether M-current suppression is involved in seizures and epileptogenesis.

Methods: Kv7.2 knock-in mice lacking the key PKC phosphorylation acceptor site for M-current suppression were generated by introducing an alanine substitution at serine residue 559 of mouse Kv7.2, mKv7.2(S559A). Basic electrophysiological properties of the M-current between wildtype and Kv7.2(S559A) knock-in mice were analyzed in primary cultured neurons. Homozygous Kv7.2(S559A) knock-in mice were used to evaluate the protective effect of mutant Kv7.2 channel against chemoconvulsant-induced seizures. In addition, pilocarpine-induced neuronal damage and spontaneously recurrent seizures were evaluated after equivalent chemoconvulsant-induced status epilepticus was achieved by coadministration of M-current specific channel inhibitor, XE991.

Result: Neurons from Kv7.2(S559A) knock-in mice showed normal basal M-currents. Knock-in mice displayed reduced M-current suppression when challenged by a muscarinic agonist, oxotremorine-M. Kv7.2(S559A) mice were resistant to chemoconvulsant-induced seizures with no mortality. Administration of XE991 transiently exacerbated seizures in knock-in mice equivalent to those of wildtype mice. Valproate, which disrupts neurotransmitter-induced M-current suppression, showed no additional anticonvulsant effect in Kv7.2(S559A) mice. After experiencing status epilepticus, Kv7.2(S559A) knock-in mice did not show seizure-induced cell death nor spontaneous recurring seizures.

[*]**Correspondence author:** Naoto Hoshi, Department of Pharmacology, University of California, Irvine, 360 Med Surge II, Irvine, CA 92697, USA, Tel: 949-824-0969, Fax: 929-824-4855, nhoshi@uci.edu.

Author contribution: DLG, AK designed, conducted, analyzed experiments and wrote the manuscript. NH designed, conducted, analyzed and supervised the experiments and wrote the manuscript.

Conflict of interest: Authors declare not conflict of interest.

Ethical publication statement: We confirm that we have read the Journal's position on issues involved in ethical publication and affirm that this report is consistent with those guidelines.

Keywords

Kv7.2; *Kcnq2*; pilocarpine; kainate; epilepsy

INTRODUCTION

Kcnq genes encode subunits of the Kv7 potassium channel family (Kv7.1–7.5). Kv7.2–7.5 subunits constitute neuronal Kv7 channels while the Kv7.1 subunit is expressed in the heart and pancreatic beta cells [1–3]. Kv7.2, Kv7.3 and Kv7.5 subunits are widely expressed in various neuronal types in both central and peripheral nervous systems, which form channels that generate a non-inactivating low-threshold voltage-gated potassium current known as the M-type potassium current or the M-current [4–7]. Although persistent changes to Kv7 channel activity by genetic mutations of the human *Kcnq2* gene are well known to be linked with various types of epilepsies [8], the role of transient modulation of Kv7 channel activities in epilepsy is not well understood.

The physiological role of basal M-current activity includes generating spike frequency adaptation [9] and setting the firing frequency of regularly firing neurons [10]. Another important physiological role of neuronal Kv7 channels is inducing transient increase in neuronal excitability in response to various neurotransmitters through M-current suppression, most notably by activation of muscarinic acetylcholine receptors (m1 or m3) [11; 12]. Despite clear demonstrations of increase in neuronal excitability *in vitro* by M-current suppression, the physiological and pathological roles of M-current suppression *in vivo* are not well understood. The major reason for this is that the regulatory mechanism of M-current suppression remained elusive until recently. Accumulating evidence suggests that the loss of phosphatidylinositol 4,5-bisphosphate (PIP2) from Kv7 subunits induces M-current suppression [13; 14] because it is an essential co-factor for ion conduction [15]. Loss of PIP2 from Kv7.2 subunit can be achieved by two mechanisms: depletion of PIP2 by phospholipase C [16] or reduction of PIP2 affinity at the Kv7.2 subunit [14]. In the latter mechanism, PKC mediated phosphorylation at serine 541 in rat Kv7.2 subunit [17; 18], which corresponds to 559 for mouse and 558 for human orthologues, dissociates calmodulin from the Kv7.2 channel complex lowering affinity of Kv7.2 subunit to PIP2 (Fig. 1A) [14].

When this key PKC phosphoacceptor serine residue in the Kv7.2 subunit is mutated to alanine, neurotransmitter-induced M-current suppression is drastically attenuated [14; 17]. We recently demonstrated that valproate treatment disrupts M-current suppression and observed that resultant preserved M-current contributes to the anticonvulsant action of valproate [19].

In support of neurotransmitter-mediated M-current suppression during seizures, microdialysis studies have shown that several neurotransmitters, including acetylcholine, become elevated during and after seizures [20; 21]. Therefore, M-current suppression during seizure episodes might be part of the seizure pathophysiology.

To address the role of M-current suppression in seizures, we generated a knock-in mouse line lacking the key PKC phosphorylation site mentioned above in the mouse *Kcnq2* gene, mKv7.2(S559A). In this paper, we analyzed wildtype and homozygous Kv7.2(S559A) mice

to elucidate whether M-current suppression exacerbates seizures and contributes to status epilepticus-induced epileptogenesis in adult animals.

MATERIALS AND METHODS

Generation of Kv7.2(S559A) mice.

Residue numbers in the mouse Kv7.2 protein in this article are based on the sequence of mouse *Kcnq2*, transcript variant 1 (NM_010611.3). Generation of the targeting vector was performed at BAC Recombineering Core, Duke Comprehensive Cancer Center (Duke University). The mutated sequence for *Kcnq2* (S559A) is as follows: gcgaaagttcaaagagGCCctgcgcccatatg (capital letters correspond to the mutated alanine residue). Homologous recombination of the targeting vector was performed at the UC Irvine Transgenic Mouse Facility using a C57BL/6NTac derived ES cell line (JM8.N4). Homologous recombination was confirmed by Southern blots. Resultant chimeric mice, were then crossed with C57BL/6-Tg(Zp3-cre)93Knw/j (Jackson Laboratory) to generate global knock-in mice. Excision of the neo cassette was confirmed by genomic PCR (Suppl. Fig. 1). Generated knock-in mice were backcrossed to C57BL/6J mice for six generations. All recombinant DNA experiments were approved by the Institutional Biosafety Committee at UC Irvine. All animal experimental procedures were approved by The Institutional Animal Care and Use Committee at UC Irvine.

Cell culture and electrophysiology.

Neuron isolation and primary neuron culture were performed according to the protocol described previously [22] with some modifications. Briefly, cortical neurons were collected from forebrains of neonatal mice (post-natal day 0), dispersed by papain (2.5 mg/ml) and DNase (100 μg/ml), and plated onto poly-D-lysine coated 35 mm dishes at 8×10^5 to 1×10^6 cells per dish. Neurons were maintained in a Neurobasal A medium containing B27, Glutamax, and 5 μM AraC (Thermo Fisher Scientific) and cultured *in vitro* for 16 to 18 days before experiments. Superior cervical ganglion (SCG) neurons were prepared from 3-week old mice and cultured for 2 to 4 days as described [23].

Perforated patch-clamp recordings were performed at room temperature on isolated primary neurons using an Axopatch 200B patch-clamp amplifier (Molecular Devices, Sunnyvale, CA, USA) as described [19]. Signals were sampled at 2 kHz, filtered at 1 kHz, and acquired using pClamp software (version 10, Molecular Devices). The perforated patch-clamp method with amphotericin B was used to record macroscopic currents as described previously [19]. Briefly, patch pipettes (1–2 MΩ) were filled with the intracellular solution containing 130 mM potassium acetate, 15 mM KCl, 3 mM $MgCl_2$, 6 mM NaCl, 10 mM HEPES (adjusted to pH = 7.2 by NaOH), and amphotericin B (0.1–0.2 mg/ml). The extracellular solution consisted of 130 mM NaCl, 3 mM KCl, 1 mM $MgCl_2$, 0.1 mM $CaCl_2$, 11 mM glucose, and 10 mM HEPES (adjusted to pH = 7.4 with NaOH). Hyperpolarizing 500-ms step pulses to −50 mV from a holding potential of −30 mV with 10 s interval were used to measure the M-current. Amplitudes of the M-currents were measured as XE991-sensitive standing current at −30 mV for cortical neurons. After establishing stable current recording for more than 2 min, 0.3 μM oxo-M was applied for 2 min, followed by 10 μM

XE991 to assess M-current suppression as well as achieve complete inhibition of the M-current. For SCG neurons, deactivating currents during −50 mV step hyperpolarization are measured as the M-current as described [19]. Dose response curve was fit using an equation I = 1-(1-Imin)/(1+ (IC50/[oxo-M])), where Imin is the resistant fraction of the M-current, IC_{50} is the half inhibition concentration and [oxo-M] is concentration of oxo-M.

Chemoconvulsant-induced seizures.

2 to 3-month-old C57BL/6 and homozygous Kv7.2(S559A) knock-in mice of both sexes were used. For pilocarpine-induced seizure experiments, methyl scopolamine (1 mg/kg i.p.) was administered 15 minutes before injecting pilocarpine (289 mg/kg i.p.) [24]. 30 minutes after pilocarpine administration, mice were injected either with 2 mg/kg XE991 (i.p.) in Dulbecco's phosphate-buffered saline (DPBS), or DPBS alone in indicated experiments [24]. Mice were video-taped for the subsequent 2 hours after pilocarpine injection, and behavior was scored by treatment and genotype-blind observers every 10 min according to a modified Racine scale with the following criteria: stage 1) immobility and facial twitching; stage 2) head bobbing, Straub tail, "wet dog shakes"; stage 3) unilateral forelimb myoclonus; stage 4) bilateral forelimb myoclonus, rearing; stage 5) total loss of balance, generalized convulsions. Animals that died during the experiments were assigned stage 5 thereafter. Status epilepticus was defined as behavioral seizures that reached stage 5 within the two-hour observation period with at least two additional incidences of stage 4 – 5 seizures. For seizure survival experiments, mice were administered diazepam (5 mg/kg i.p.) two hours after pilocarpine injection to terminate seizures and were given 5% glucose infusions until body weight was stabilized to correct dehydration.

For kainate-induced seizure experiments, one hour after kainate administration injected subcutaneously at indicated doses, mice were injected either with 2 mg/kg XE991 (i.p.) in DPBS, or DPBS alone in indicated experiments. For VPA experiments, adult mice were administered either freshly prepared sodium valproate (250 mg/kg, VPA. i.p.) or physiological saline solution twice daily for 3.5 days [19]. Kainate was administered at least 6 hours after the final VPA administration. To evaluate behavioral seizures, mice were videotaped for the subsequent 4 hours after kainate injection, and behavior was scored by treatment and genotype blind observers every 10 minutes according to a previously described modified Racine scale [19] with the following criteria: stage 1) immobility; stage 2) rigidity; stage 3) automatisms with scratching, head bobbing and circling; stage 4) intermittent rearing and falling; stage 5) continuous rearing and falling; stage 6) tonic-clonic whole body convulsions and rapid jumping. All mice that died during the experiments were assigned stage 6 thereafter.

Spontaneously recurrent seizures.

Pilocarpine-experienced wildtype and Kv7.2(S559A) mice that underwent status epilepticus were selected for observation of development of spontaneous ictal activity. Three weeks after induction of status epilepticus animals were videotaped for 3 hours/day for 15 days and observed by a treatment and genotype blind observer. Episodes with ≥ stage 4 seizure were considered to have a seizure and the frequency of ictal activity was logged.

Immunohistochemistry.

Immunohistochemistry protocol was followed as previously described [19]. 2 h after injection of pilocarpine, deeply anesthetized mice were fixed by 4% paraformaldehyde perfusion. c-Fos expression was detected using a rabbit anti-c-Fos antibody (1:1000 dilution, Cat No. PC38; Calbiochem). GAD 67 was detected by anti-GAD67 antibody (1:5000 dilution, Cat. No. MAR5406; EMD Millipore). VECTASHIELD with DAPI (Vector Laboratories) was used for mounting. Immunofluorescent images were acquired using a fluorescent light microscope (Leica, DM4000B) equipped with a CCD camera (Optronics MicroFire, OPTMIF). Fluorescent images were quantified by observers blind to genotype and treatment using MetaMorph (Molecular Devices).

Degenerating neurons were labeled by incubation with 0.0001% Fluoro Jade C (Cat. No. 1FJC; Histo-Chem Inc.) dissolved in 0.1% acetic acid for 20 minutes. FJC images of whole sections were generated using a fluorescent light microscope (BZ-9000, Keyence).

Statistics.

All results are expressed as the mean ± s.e.m. Statistical significance of the results was assessed by non-parametric analysis of variance (Kruskal-Wallis test) followed by Dunn's multiple comparisons test or Mann-Whitney test performed by Prism 6 (GraphPad, La Jolla, CA). $P < 0.05$ was considered significant.

Results

Non-inactivating currents in neurons from Kv7.2(S559A) mice.

We introduced an alanine substitution at the key PKC phosphorylation site [17] in the mouse *Kcnq2* gene (Fig. 1A), Kv7.2(S559A), and generated Kv7.2(S559A) knock-in mice. The residue at this phosphorylation site is conserved throughout the Kv7 subfamily except for the non-neuronal Kv7.1 subunit. Homologous recombination in embryonic stem cells was confirmed by Southern blotting (Supple. Fig.1). In clear contrast to global *Kcnq2* knock-out mice that are neonatal lethal due to pulmonary atelectasis [25] or conditional *Kcnq2* knock-out mice that show premature death due to seizures [26], these Kv7.2(S559A) knock-in mice showed normal growth with no premature death (Supple. Fig.1).

We examined basic electrophysiological properties of primary cultured cortical neurons from Kv7.2(S559A) mice. To minimize rundown of the M-current during measurements we used the amphotericin B perforated patch technique. Cells were held at a holding potential of −30 mV to inactivate most voltage-gated channels and 1-s test potentials between −120 mV and +10 mV were applied to measure remaining non-inactivating currents (Fig 1A). Obtained I-V responses from neurons were almost identical between wildtype and Kv7.2(S559A) mice (Fig 1B & C). In addition, there were no differences in membrane capacitances [46.5 ± 3.3 pF for wt (n = 27), 46.2 ± 4.0 pF for Kv7.2(S559A) (n = 24)], or input resistance near the resting membrane potential at −70 mV [218 ± 18 MΩ for wt, 201 ± 20 MΩ for K7.2 (S559A)]. These results suggest that expression of Kv7.2(S559A) subunits did not cause significant changes in biophysical properties of these neurons.

We next focused on the M-current and M-current suppression in cultured cortical neurons. Cells were held at −30 mV and conductance was monitored by a 500-ms step hyperpolarization to −50 mV. After stable recordings were established, 0.3 μM oxotremorine-M (oxo-M) was applied to measure M-current suppression, followed by 10 μM XE991 for full inhibition of the M-current (Fig 1D). M-current was measured as XE991-sensitive standing current at −30 mV since XE991 is a Kv7 channel selective inhibitor. 0.3 μM oxo-M suppressed the M-current to 56.7 ± 4.3% (n = 9) in neurons from wildtype control. In contrast, neurons from Kv7.2(S559A) showed little M-current suppression, and M-currents were preserved at 89.1 ± 6.3% (n = 10) in the presence of oxo-M ($P < 0.01$, Mann Whitney test). Similar results were obtained from SCG neurons (Suppl. Fig 1F & G). Next, dose response experiments were conducted to evaluate M-current suppression at various agonist concentrations (Fig. 1E). The dose response curve showed IC_{50} of 0.32 ± 0.02 μM and Imin of 0.1 ± 0.01 for wildtype control. In contrast, that from Kv7.2(S559A) mice showed IC_{50} of 1.28 ± 0.08 μM and Imin of 0.35 ± 0.01. These results suggest that the M-current in Kv7.2(S559A) mice requires higher concentration of oxo-M for suppression with an increased resistant fraction. These results indicate that we have generated Kv7.2 mutant knock-in mice that have diminished M-current suppression while retaining normal basal M-current activity.

Protective phenotype of Kv7.2(S559A) mice against chemoconvulsant-induced seizures.

Since a muscarinic agonist, pilocarpine, is widely used to induce experimental seizures [27], we first tested pilocarpine-induced seizures to examine whether diminished M-current suppression has any effect on seizures. In wildtype mice, pilocarpine injection (289 mg/kg pilocarpine, i.p.) caused persistent behavioral seizures reaching to the maximal stage 5 in a modified Racine scale, whereas the maximal seizure stage for most of the homozygous Kv7.2(S559A) mice tested peaked at stage 3 ($p < 0.01$, Fig 2). Mortality in pilocarpine injected mice was 3/9 for wildtype mice, and 0/5 for Kv7.2(S559A) mice. To examine whether this resistance to pilocarpine is due to the preserved M-current during seizures, we administered XE991 (2 mg/kg, i.p.) 30 min after pilocarpine injection. After administration of XE991 to Kv7.2(S559A) mice, pilocarpine-induced seizures reached stage 5, equivalent to that of wildtype control, and the effect gradually diminished after one hour (Fig 2B and C).

To examine whether the resistance of Kv7.2(S559A) mice to chemoconvulsants is limited to seizures induced by muscarinic agonists, we next tested kainate. Kainate receptors are ionotropic receptors that depolarize membrane potentials in neurons and are widely used to induce experimental seizures [28]. Administration of kainate (30 mg/kg, s.c.) induced severe seizures in wildtype control mice, most of which reached the maximal seizure, stage 6, while inducing milder stage 3 seizures in Kv7.2(S559A) mice, as shown in Fig. 2D ($p < 0.001$). In addition, mortality was 8/12 for wildtype and 0/13 for Kv7.2(S559A) mice ($P < 0.001$, two-tailed Fisher's exact test). Similarly to pilocarpine-induced seizures, resistance to kainate was transiently abolished by administration of XE991 (Fig 2E & F). These results suggest that disruption of M-current suppression by Kv7.2(S559A) mutant channels attenuates behavioral seizures and increases survival rate in these chemoconvulsant-induced seizures.

We previously demonstrated that preservation of the M-current contributes to the non-acute anticonvulsant effect of valproate (VPA) [19], theoretically through a similar mechanism to that of the Kv7.2(S559A) mutation. Therefore, we tested whether VPA effects were occluded in Kv7.2(S559A) mice in the kainate seizure model. A three-day treatment with VPA (500 mg/kg/day), with which we observed protective effects in wildtype mice against kainate seizures [19], did not show any effect in Kv7.2(S559A) mice (Fig 3A). In contrast, diazepam (5 mg/kg, i.p.), which targets GABA receptors, further suppressed behavioral seizures in Kv7.2(S559A) mice (Fig 3B & C). These results suggest that the Kv7.2(S559A) mutation and VPA treatment use the same pathway for their anticonvulsant effects.

Effects of the Kv7.2(S559A) mutation against seizure-induced neuronal damage and epileptogenesis.

Our results so far indicate that preserved Kv7.2 channel activity by Kv7.2(S559A) mutation has anticonvulsant effects. Another important question is whether disruption of M-current suppression is involved in epileptogenesis. One hypothesis for epileptogenesis is that brain damage caused by an initial severe seizure induces remodeling of neuronal circuits, which leads to spontaneously recurrent seizures [29]. Pilocarpine-induced status epilepticus was used for this experiment since C57BL/6 mice are resistant to neurodegeneration after kainate-induced seizures [30]. We used the condition shown in Fig 2 with XE991 injection (2mg/kg, i.p.) at 30 min after pilocarpine administration to deliver equivalent status epilepticus in Kv7.2(S559A) and wildtype mice (Supple. Fig.2). To evaluate whether both groups underwent equivalent neural excitation, induction of c-Fos was examined by immunohistochemistry in the hippocampus (Fig 4). In wildtype mice, administration of pilocarpine as well as pilocarpine+XE991 induced significant c-Fos expression in the CA1 region and the dentate gyrus (Fig 4). In contrast, pilocarpine administration alone did not induce c-Fos expression in Kv7.2(S559A) mice (Fig 4) as was predicted from milder seizures (Supple. Fig.2). In contrast, XE991 administration during pilocarpine-induced seizures exacerbated seizures in Kv7.2(S559A) mice (Supple. Fig.2) and induced c-Fos expression equivalent to that of wildtype mice with status epilepticus (Fig 4). For both genotypes, c-Fos positive cells were predominantly pyramidal neurons in the CA1 region, and those in the dentate gyrus were found both in the granule cell layer and in the hilus (Fig 4).

A separate cohort was used to determine seizure-induced neurodegeneration. Neuronal damage was assessed by Fluoro Jade C staining (FJC) two days after initial status epilepticus using the same pilocarpine+XE991 protocol (Supple. Fig.2). We found prominent FJC positive neurons in various brain regions including the CA1 region and the dentate gyrus of the wildtype control (Fig 5 and Supple. Fig. 3). The majority of FJC positive cells were pyramidal neurons in the CA1 region and neurons in the hilus of the dentate gyrus (Fig 5). Interestingly, even though granule neurons showed apparent c-Fos induction (Fig 4), there was minimal FJC staining in granule neurons (Fig 5). For Kv7.2(S559A) mice, we detected nominal FJC positive neurons throughout the brain including these two brain regions, which were not significantly different from the negative control (Fig 5 and Supple. Fig. 3). These results suggest that the Kv7.2(S559A) mutation has neuroprotective effects against pilocarpine-induced status epilepticus.

Spontaneous recurrent seizures after pilocarpine-induced status epilepticus are widely used as a model for temporal epilepsy [27]. Therefore, we examined the occurrence of spontaneously recurrent seizures in wildtype and Kv7.2(S559A) mice three weeks after pilocarpine-induced status epilepticus using the pilocarpine+XE991 protocol. Cumulative seizure stage suggested that both groups underwent equivalent status epilepticus (Supple. Fig.2). Three weeks later, we examined for the occurrence of spontaneous seizures during 3-h observation periods for 15 consecutive days. In the wildtype control mice, we detected recurrent behavioral seizures on 5.7 ± 0.7 days in 10/11 mice (Fig 6A), which lasted 70 ± 0.2 s. The remaining wildtype mouse showed seizures only during one observation period. In contrast, Kv7.2(S559A) mice showed no recurrent spontaneous seizures (0/10, $P < 0.0001$, Mann Whitney test, Fig 6A). Only a single seizure episode was detected in one Kv7.2(S559A) mouse, which lasted 125 s. To examine epileptogenic changes in these mice, we conducted GAD67 immunostaining since reduction of GABAergic neurons is implicated in epileptogenesis [24]. GAD67 immunoreactivity was reduced in status epilepticus-experienced wildtype mice compared to naive control wildtype mice (Fig. 6B). In contrast, such reduction was not observed in status epilepticus-experienced Kv7.2(S559A) mice (Fig 6B–C). Spontaneously recurrent seizures and GAD67 immunoreactivity suggest epileptogenic changes were averted in Kv7.2(S559A) mice.

DISCUSSION

We generated Kv7.2(S559A) knock-in mice that exhibit normal growth and no premature death, suggesting that M-current suppression is not required for basic life supporting behaviors. Furthermore, we demonstrated that Kv7.2(S559A) knock-in mice have milder seizures in both kainate and pilocarpine-induced seizure models. In addition, mortality in both chemoconvulsant-induced seizure models was suppressed in Kv7.2(S559A) mice in the conditions used in this study. Because XE991 administration exacerbates seizures in Kv7.2(S559A) mice to the level of wildtype mice, resistance to chemoconvulsant-induced seizures in Kv7.2(S559A) mice is most likely attributed to preservation of the M-current during seizures. This result supports our view that the anticonvulsant mechanism of action for valproate is critically dependent on this phosphoacceptor residue during seizures [19].

Since M-current regulates the tone of neural firing, it may not be surprising that M-current suppression facilitates neural firing during seizures. However, whether prompt restoration of M-current after seizures has any therapeutic benefits is an open question. XE991 selectively exacerbates seizures in Kv7.2(S559A) mice, which lasts around one hour as shown in Fig 2. This duration of XE991 effect is consistent with published pharmacokinetic studies [31; 32]. In addition, our recent study shows that XE991 is an irreversible inhibitor for Kv7 channels, suggesting that recovery is due to removal of XE991 from the system rather than washout of XE991 from Kv7 channels [33]. Our FJC staining results suggest that recovery of M-current after XE991 effect, which occurs after status epilepticus, is still sufficient to prevent neuronal degeneration. Nonetheless, the neuroprotective effects in Kv7.2(S559A) mice were unexpected because we initially assumed that post-seizure neuronal degeneration was due to excitotoxicity as a result of status epilepticus. One caveat to this conclusion is whether Kv7.2(S559A) mice indeed underwent status epilepticus equivalent to that of wildtype control mice. However, we think that it is highly likely that both groups experienced

equivalent status epilepticus for the following reasons, 1) c-Fos immunohistochemistry showed equivalent expression in XE991-treated groups (Fig 4), and 2) both groups showed equivalent cumulative seizure stages (Supple. Fig.2). On the other hand, our experimental design is not able to elucidate whether M-current suppression after status epilepticus takes the form of sustained suppression or repetitive suppression. In addition, it will be important to determine the critical period of this protective effect. These issues should be addressed in future studies.

Our results provide evidence for the involvement of M-current suppression during seizure; however, this study presents some limitations to be addressed. 1) Characterization of the M-current was conducted in cultured neurons, use of brain slice electrophysiology will provide an environment more closely resembling neuromodulation *in vivo* [34–36]. 2) While there is an inherent lack of behavioral seizures in Kv7.2(S559A) mice using the pilocarpine model of acquired epilepsy, future inclusion of EEG will provide more definite proof of the absence of ictal activities following SE. 3) The timing and extent of M-current suppression *in vivo* are currently unknown, which will provide future direction for determining the aforementioned critical period of M-current suppression responsible for its contribution to epileptogenesis.

In summary, M-current suppression not only exacerbates seizures but also contributes to neuronal degeneration and epileptogenesis in mouse. Therefore, prompt restoration of Kv7.2 channel function after seizures may provide long-term therapeutic benefits and should be explored further.

Supplementary Material

Refer to Web version on PubMed Central for supplementary material.

Acknowledgement:

This work is supported in part by a NIH grant NS067288.

References

1. Jentsch TJ. Neuronal KCNQ potassium channels: physiology and role in disease. Nat Rev Neurosci 2000;1:21–30. [PubMed: 11252765]
2. Brown DA, Passmore GM. Neural KCNQ (Kv7) channels. Br J Pharmacol 2009;156:1185–1195. [PubMed: 19298256]
3. Greene DL, Hoshi N. Modulation of Kv7 channels and excitability in the brain. Cell Mol Life Sci 2016.
4. Brown BS, Yu SP. Modulation and genetic identification of the M channel. Prog Biophys Mol Biol 2000;73:135–166. [PubMed: 10958929]
5. Robbins J KCNQ potassium channels: physiology, pathophysiology, and pharmacology. Pharmacol Ther 2001;90:1–19. [PubMed: 11448722]
6. Wang HS, Pan Z, Shi W, et al. KCNQ2 and KCNQ3 potassium channel subunits: molecular correlates of the M-channel. Science 1998;282:1890–1893. [PubMed: 9836639]
7. Fidzinski P, Korotkova T, Heidenreich M, et al. KCNQ5 K(+) channels control hippocampal synaptic inhibition and fast network oscillations. Nat Commun 2015;6:6254. [PubMed: 25649132]
8. Miceli F, Soldovieri MV, Joshi N, et al. KCNQ2-Related Disorders. In Adam MP, Ardinger HH, Pagon RA, et al. (Eds) GeneReviews((R)): Seattle (WA); 2016.

9. Delmas P, Brown DA. Pathways modulating neural KCNQ/M (Kv7) potassium channels. Nat Rev Neurosci 2005;6:850–862. [PubMed: 16261179]
10. Lawrence JJ, Saraga F, Churchill JF, et al. Somatodendritic Kv7/KCNQ/M channels control interspike interval in hippocampal interneurons. J Neurosci 2006;26:12325–12338. [PubMed: 17122058]
11. Brown DA, Adams PR. Muscarinic suppression of a novel voltage-sensitive K+ current in a vertebrate neurone. Nature 1980;283:673–676. [PubMed: 6965523]
12. Fukuda K, Higashida H, Kubo T, et al. Selective coupling with K+ currents of muscarinic acetylcholine receptor subtypes in NG108–15 cells. Nature 1988;335:355–358. [PubMed: 2843772]
13. Suh BC, Inoue T, Meyer T, et al. Rapid chemically induced changes of PtdIns(4,5)P2 gate KCNQ ion channels. Science 2006;314:1454–1457. [PubMed: 16990515]
14. Kosenko A, Kang S, Smith IM, et al. Coordinated signal integration at the M-type potassium channel upon muscarinic stimulation. EMBO J 2012;31:3147–3156. [PubMed: 22643219]
15. Hansen SB, Tao X, MacKinnon R. Structural basis of PIP2 activation of the classical inward rectifier K+ channel Kir2.2. Nature 2011;477:495–498. [PubMed: 21874019]
16. Suh BC, Hille B. PIP2 is a necessary cofactor for ion channel function: how and why? Annu Rev Biophys 2008;37:175–195. [PubMed: 18573078]
17. Hoshi N, Zhang JS, Omaki M, et al. AKAP150 signaling complex promotes suppression of the M-current by muscarinic agonists. Nat Neurosci 2003;6:564–571. [PubMed: 12754513]
18. Hoshi N, Langeberg LK, Scott JD. Distinct enzyme combinations in AKAP signalling complexes permit functional diversity. Nat Cell Biol 2005;7:1066–1073. [PubMed: 16228013]
19. Kay HY, Greene DL, Kang S, et al. M-current preservation contributes to anticonvulsant effects of valproic acid. J Clin Invest 2015;125:3904–3914. [PubMed: 26348896]
20. Zis AP, Nomikos GG, Brown EE, et al. Neurochemical effects of electrically and chemically induced seizures: an in vivo microdialysis study in the rat hippocampus. Neuropsychopharmacology 1992;7:189–195. [PubMed: 1382432]
21. Baptista T, Weiss SR, Zocchi A, et al. Electrical kindling is associated with increases in amygdala acetylcholine levels: an in vivo microdialysis study. Neurosci Lett 1994;167:133–136. [PubMed: 8177511]
22. Kaech S, Banker G. Culturing hippocampal neurons. Nat Protoc 2006;1:2406–2415. [PubMed: 17406484]
23. Tunquist BJ, Hoshi N, Guire ES, et al. Loss of AKAP150 perturbs distinct neuronal processes in mice. Proc Natl Acad Sci U S A 2008;105:12557–12562. [PubMed: 18711127]
24. Hunt RF, Girskis KM, Rubenstein JL, et al. GABA progenitors grafted into the adult epileptic brain control seizures and abnormal behavior. Nat Neurosci 2013;16:692–697. [PubMed: 23644485]
25. Watanabe H, Nagata E, Kosakai A, et al. Disruption of the epilepsy KCNQ2 gene results in neural hyperexcitability. J Neurochem 2000;75:28–33. [PubMed: 10854243]
26. Soh H, Pant R, LoTurco JJ, et al. Conditional deletions of epilepsy-associated KCNQ2 and KCNQ3 channels from cerebral cortex cause differential effects on neuronal excitability. J Neurosci 2014;34:5311–5321. [PubMed: 24719109]
27. Curia G, Longo D, Biagini G, et al. The pilocarpine model of temporal lobe epilepsy. J Neurosci Methods 2008;172:143–157. [PubMed: 18550176]
28. Kainate Ben-Ari Y. and Temporal Lobe Epilepsies: 3 decades of progress. In Noebels JL, Avoli M, Rogawski MA, et al. (Eds) Jasper's Basic Mechanisms of the Epilepsies: Bethesda (MD); 2012.
29. Rakhade SN, Jensen FE. Epileptogenesis in the immature brain: emerging mechanisms. Nat Rev Neurol 2009;5:380–391. [PubMed: 19578345]
30. McLin JP, Steward O. Comparison of seizure phenotype and neurodegeneration induced by systemic kainic acid in inbred, outbred, and hybrid mouse strains. Eur J Neurosci 2006;24:2191–2202. [PubMed: 17074044]
31. Earl RA, Zaczek R, Teleha CA, et al. 2-Fluoro-4-pyridinylmethyl analogues of linopirdine as orally active acetylcholine release-enhancing agents with good efficacy and duration of action. J Med Chem 1998;41:4615–4622. [PubMed: 9804701]

32. Zaczek R, Chorvat RJ, Saye JA, et al. Two new potent neurotransmitter release enhancers, 10,10-bis(4-pyridinylmethyl)-9(10H)-anthracenone and 10,10-bis(2-fluoro-4-pyridinylmethyl)-9(10H)-anthracenone: comparison to linopirdine. J Pharmacol Exp Ther 1998;285:724–730. [PubMed: 9580619]

33. Greene DL, Kang S, Hoshi N. XE991 and Linopirdine Are State-Dependent Inhibitors for Kv7/KCNQ Channels that Favor Activated Single Subunits. J Pharmacol Exp Ther 2017;362:177–185. [PubMed: 28483800]

34. Etxeberria A, Aivar P, Rodriguez-Alfaro JA, et al. Calmodulin regulates the trafficking of KCNQ2 potassium channels. FASEB J 2008;22:1135–1143. [PubMed: 17993630]

35. Alaimo A, Gomez-Posada JC, Aivar P, et al. Calmodulin activation limits the rate of KCNQ2 K+ channel exit from the endoplasmic reticulum. J Biol Chem 2009;284:20668–20675. [PubMed: 19494108]

36. Jiang L, Kosenko A, Yu C, et al. Activation of m1 muscarinic acetylcholine receptor induces surface transport of KCNQ channels through a CRMP-2-mediated pathway. J Cell Sci 2015;128:4235–4245. [PubMed: 26446259]

Significance

This study provides evidence that neurotransmitter-induced suppression of M-current generated by Kv7.2 containing channels exacerbates behavioral seizures. In addition, prompt recovery of M-current after status epilepticus prevents subsequent neuronal death and the development of spontaneously recurrent seizures. Therefore, prompt restoration of M-current activity may have a therapeutic benefit for epilepsy.

Key point box:

1. M-current suppression during seizures exacerbated behavioral seizures.
2. Disrupting M-current suppression prevented mortality in pilocarpine or kainate-induced seizures.
3. M-current suppression after status epilepticus contributes to subsequent neuronal death.
4. Disrupting M-current suppression after status epilepticus prevented epileptogenesis.

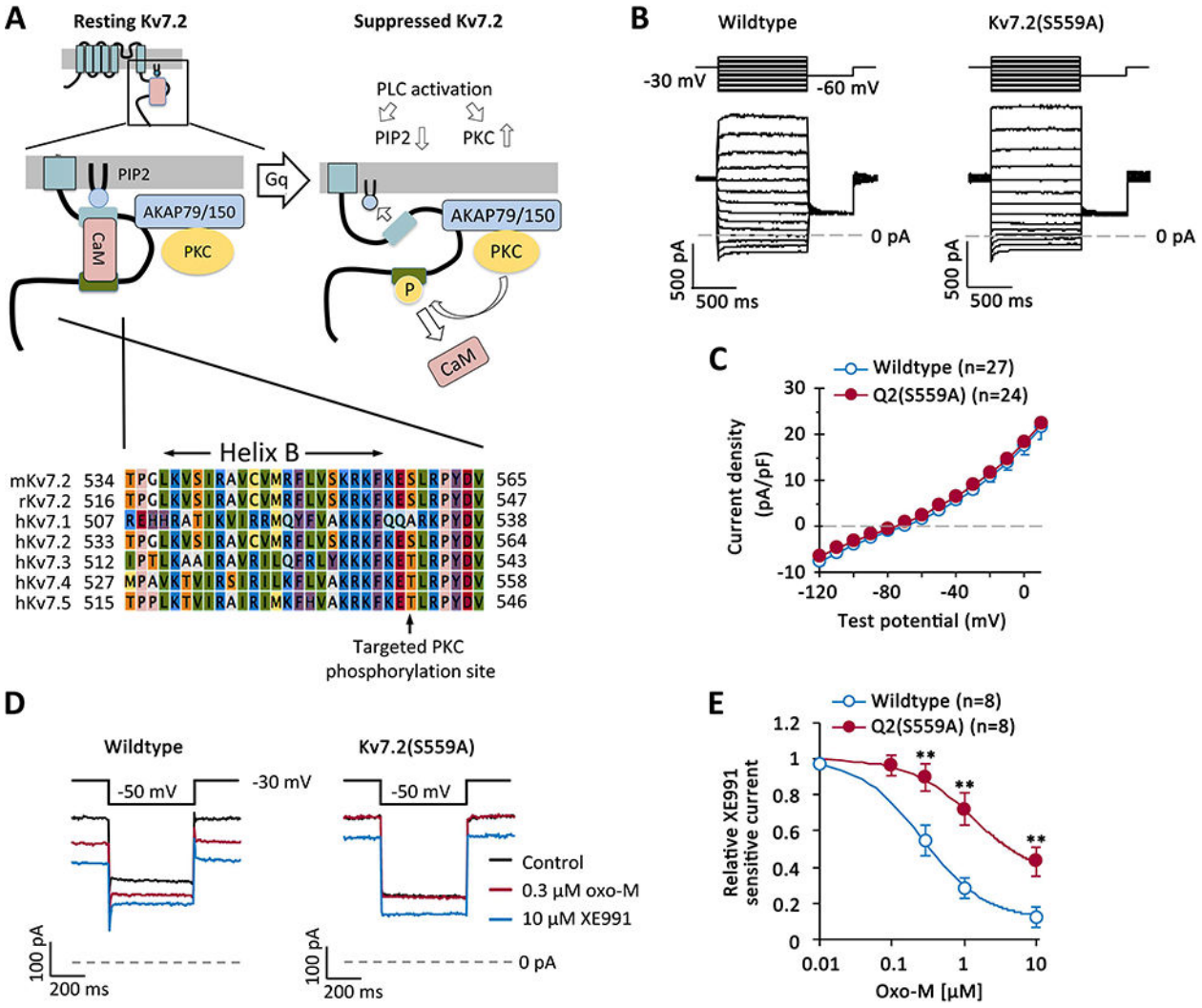

Figure 1. Schematic summary of Kv7.2 subunit composition and characterization of non-inactivating voltage-activated currents in cortical primary cultured neurons from Kv7.2(S559A) mice.

A) Schematic summary of Kv7.2 subunit and associated signaling molecules modified from reference [14]. The C-terminal tail of Kv7.2 subunit binds to phosphatidylinositol 4,5-bisphosphate (PIP2), calmodulin (CaM), and AKAP79/150 that anchors protein kinase C (PKC) at the resting state. When Gq-coupled receptor is activated, AKAP79/150 anchored PKC phosphorylates Kv7.2 subunit within the CaM binding site near the Helix B and dissociates CaM (right panel). Alignment of the Helix B and the mutated phosphorylation site in this study, mKv7.2(S559), is indicated. Mouse (m), rat (r) and human (h) Kv7 subfamilies are shown. **B)** Voltage-clamp traces showing voltage responses in neurons from wildtype and Kv7.2(S559A) mice. Voltage commands are indicated. Cells were held at −30 mV and various 1-s steps between −120 mV and +10 mV in 10 mV increments were applied. **C)** Summary of experiments in B showing no difference in the current density of voltage-activated currents in both genotypes. **D)** Representative voltage-clamp traces showing oxo-M (0.3 µM) induced suppression and XE991 (10 µM) inhibition in neurons from wildtype and Kv7.2(S559A) mice. **E)** Dose response curve showing diminished

muscarinic suppression of XE991-sensitive currents in Kv7.2(S559) neurons. ** shows $P < 0.01$ by Mann-Whitney test. Results are shown as mean ± sem.

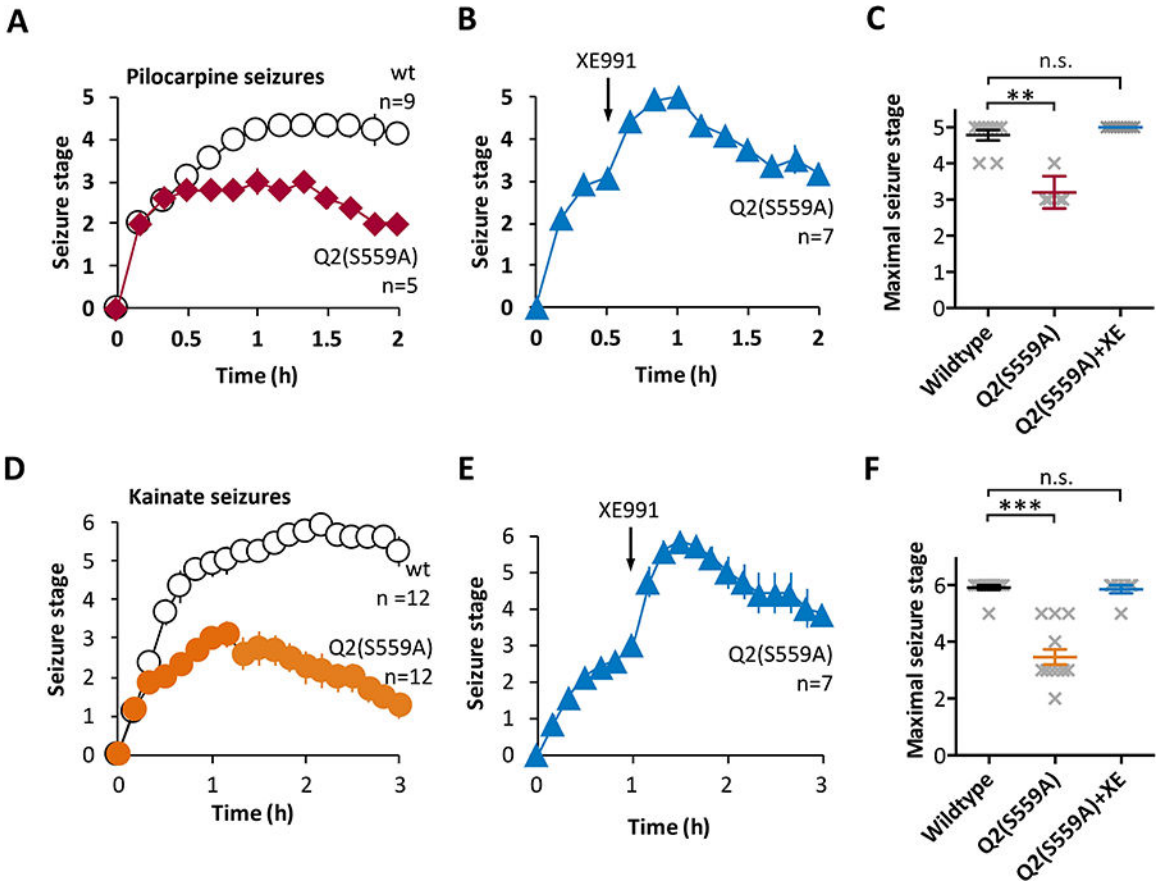

Figure 2. Chemoconvulsant-induced seizures in Kv7.2(S559A) mice.

A) Time course of pilocarpine-induced seizures (289 mg/kg) in wildtype (wt), and Kv7.2(S559A) (Q2 (S559A)) mice. Pilocarpine is injected at t = 0. **B)** XE991 (2 mg/kg) transiently exacerbated pilocarpine seizure in Kv7.2(S559A) mice at t = 0.5 h indicated by an arrow. **C)** Summary of experiments shown in A and B. X shows maximal seizure stage of each mouse. ** shows $P < 0.01$ by Non-parametric ANOVA (Kruskal-Wallis test) followed by Dunn's multiple comparisons tests. **D)** Time course of kainate-induced seizures (30 mg/kg). **E)** XE991 (2 mg/kg) transiently exacerbated kainate seizure in Kv7.2(S559A) mice. **F)** Summary of experiments shown in D and E. X shows maximal seizure stage of each mouse. *** shows $P < 0.001$ by Non-parametric ANOVA (Kruskal-Wallis test) followed by Dunn's multiple comparisons tests. Results are shown as mean ± sem.

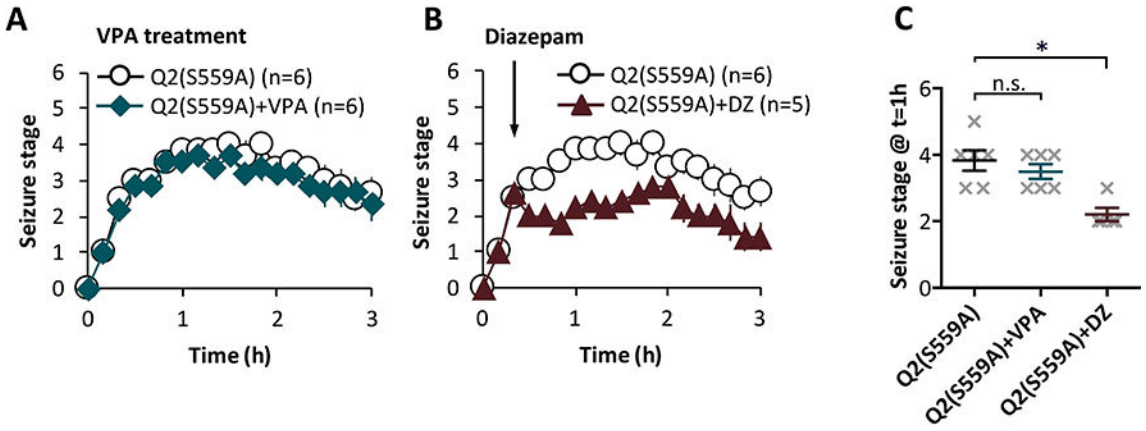

Figure 3. Diazepam but not valproate had additional anticonvulsant effects in Kv7.2(S559A) mice.

A) Valproate (VPA) had no effect on Kv7.2(S559A) mice in kainate (35 mg/kg) induced seizures. VPA (500 mg/day) was administered for three days prior to kainate injection. **B)** Diazepam (5 mg/kg) injection at t = 30 min suppressed behavioral seizures in Kv7.2(S559A) mice. **C)** Summary showing maximal seizure stages of individual mice at t = 1h shown in A and B. X represents each mouse. * shows $P < 0.05$ by Non-parametric ANOVA (Kruskal-Wallis test) followed by Dunn's multiple comparisons tests. Error bars show sem.

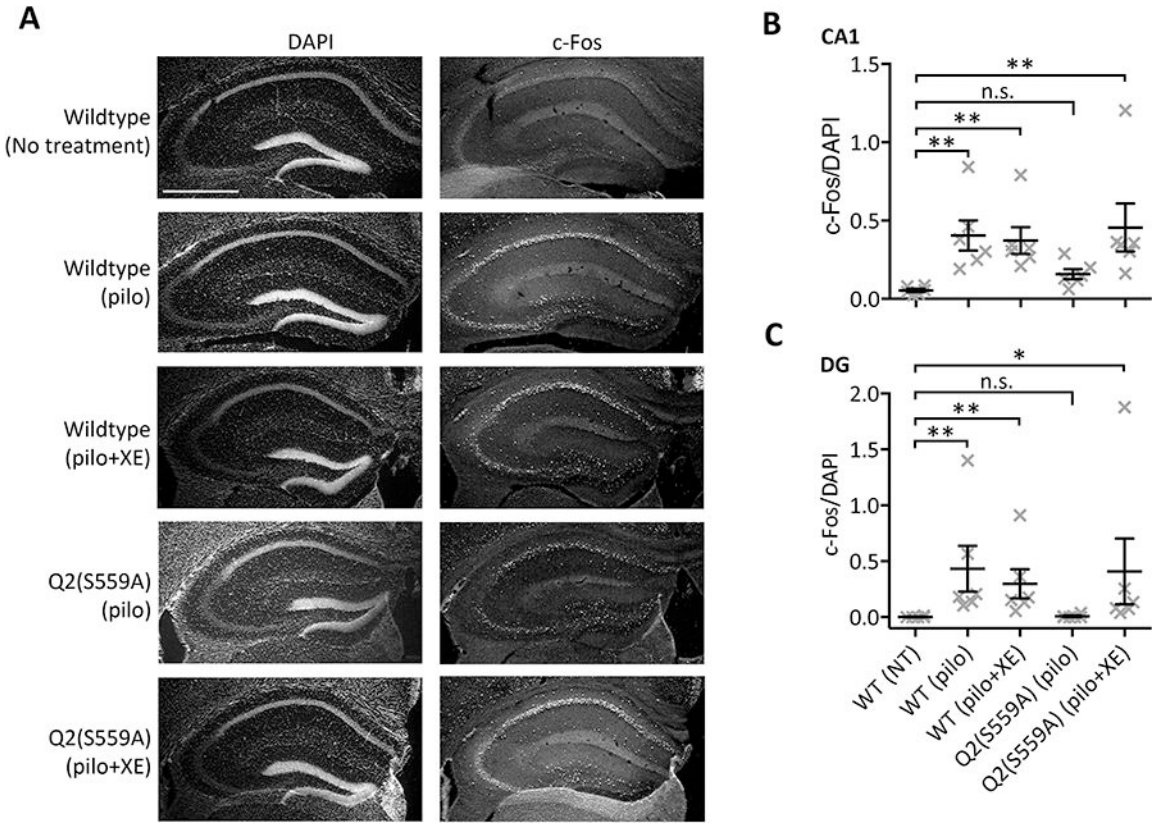

Figure 4. c-Fos induction after pilocarpine seizures in Kv7.2(S559A) mice.

A) DAPI staining and c-Fos immunofluorescent images of the hippocampus two hours after pilocarpine (289 mg/kg) injection. Scale bar shows 1 mm. **B)** Summary showing c-Fos expression in the CA1 region relative to DAPI fluorescent intensity. **C)** Summary showing c-Fos expression in the dentate gyrus relative to DAPI fluorescent intensity. X represents each mouse. *<0.05, ** < 0.01 by Non-parametric ANOVA (Kruskal-Wallis test) followed by Dunn's multiple comparisons tests. Error bars show sem.

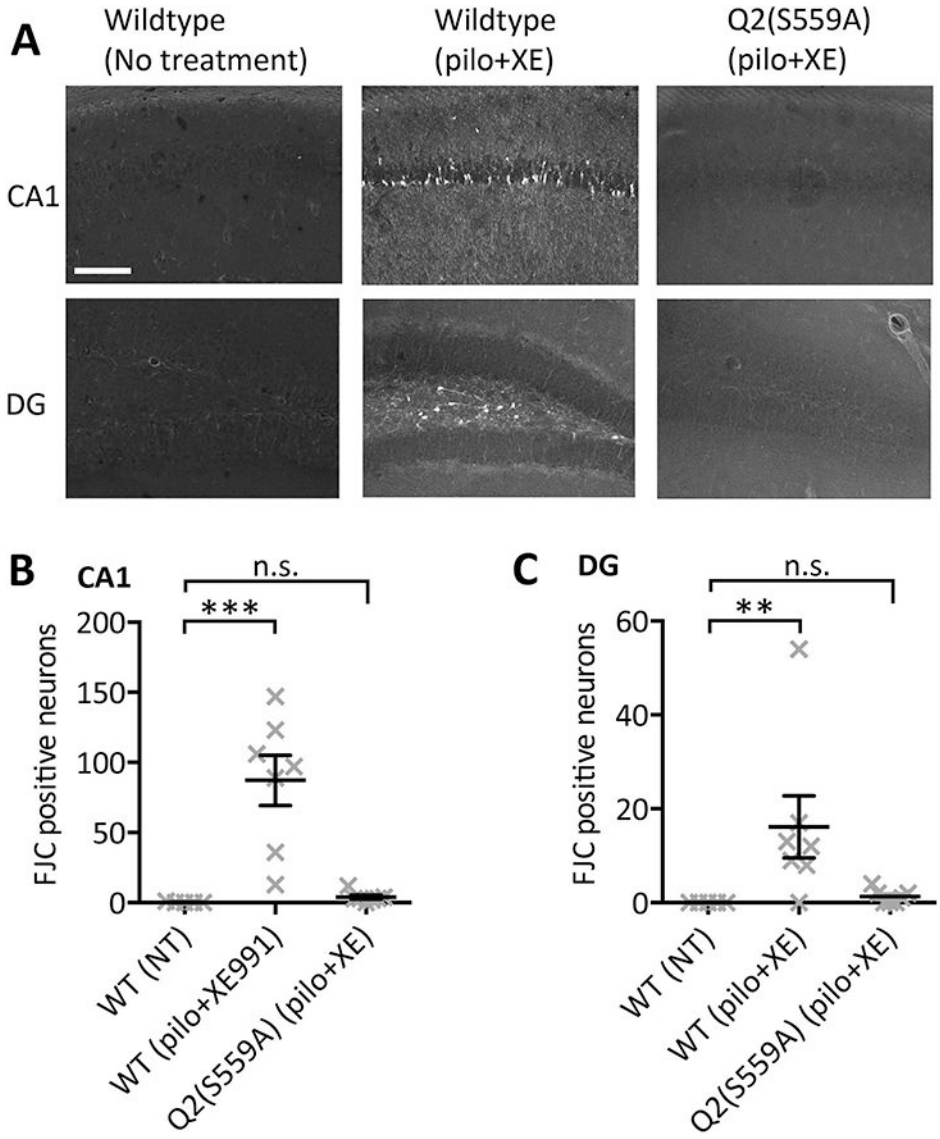

Figure 5. Neuronal damage after pilocarpine-induced status epilepticus.

A) Fluoro Jade C staining (FJC) of the CA1 region and dentate gyrus of non-treated control wildtype mice, pilocarpine+XE991 (pilo+XE) treated wildtype, and pilocarpine +XE991treated Kv7.2(S559A) mice. Scale bar shows 200 μm. **B)** Summary of FJC positive cells in the CA1 region. **C)** Summary of FJC positive cells in the dentate gyrus (DG). X represents each mouse. ** < 0.01. *** < 0.001 by Non-parametric ANOVA (Kruskal-Wallis test) followed by Dunn's multiple comparisons tests. Error bars show sem.

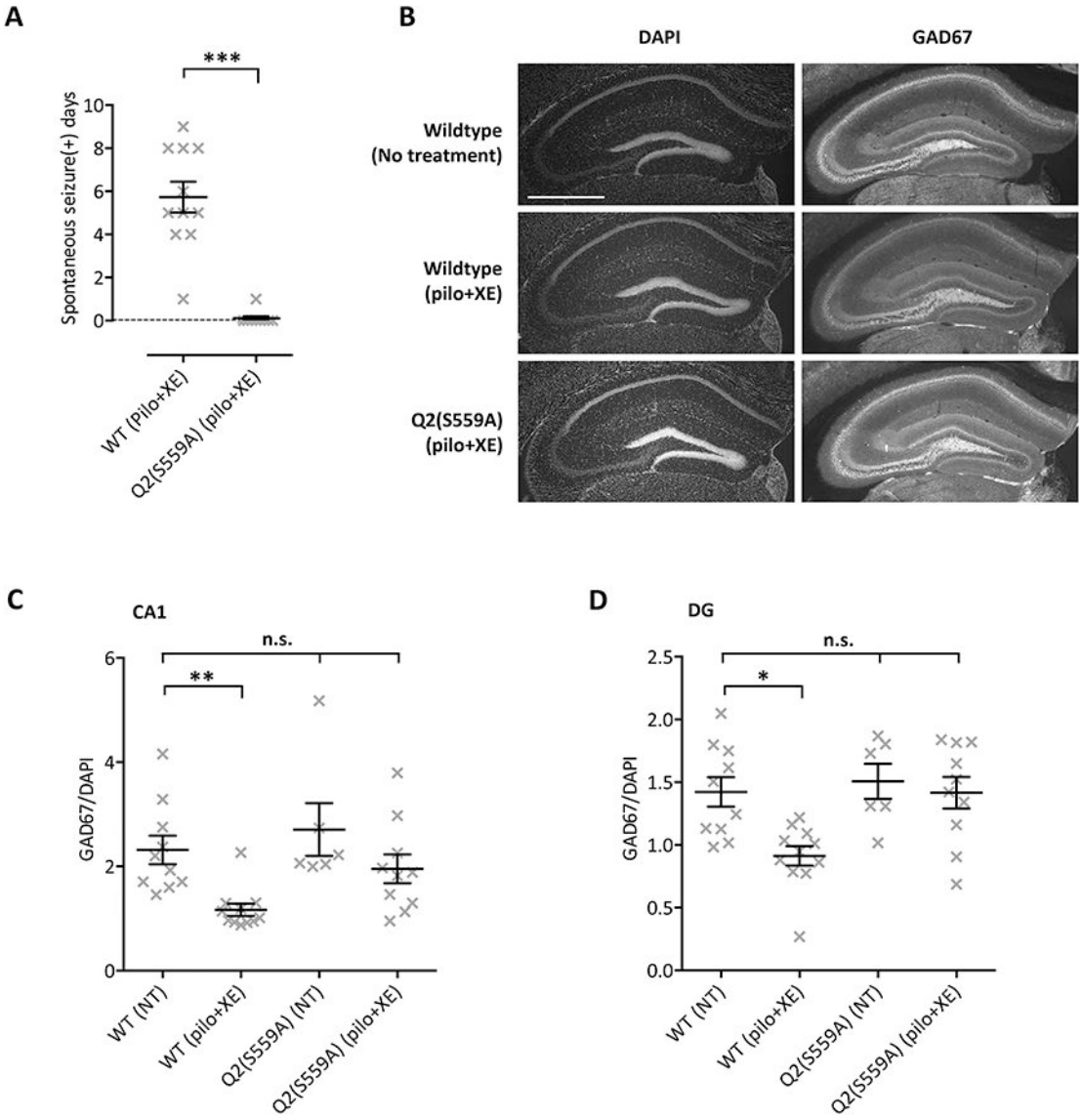

Figure 6. Spontaneous behavioral seizures and GAD67 immunoreactivity after pilocarpine-induced status epilepticus.

A) Occurrence of spontaneous behavioral seizures three weeks after pilocarpine-induced status epilepticus during a 15-day observation period. n = 11 for wildtype and n = 10 for Kv7.2(S559A) mice. *** < 0.001 by Mann-Whitney test. **B)** Representative DAPI staining and GAD67 immunofluorescent images from mice evaluated in A. Scale bar shows 1 mm. **C)** Summary showing relative GAD67 immunoreactivity of the CA1 region to DAPI signal. **D)** Summary showing relative GAD67 immunoreactivity of the dentate gyrus to DAPI signal. X represents each mouse. * < 0.05, ** < 0.01 by Non-parametric ANOVA (Kruskal-Wallis test) followed by Dunn's multiple comparisons tests. Error bars show sem.